COLLECTION OF CHARGED PARTICLES ON PROBE IN HIGH PRESSURE PLASMA

TAKAYOSHI OKUDA

Department of Electronics

(Received May 22, 1963)

Abstract

In this paper, the collection of charged particles on a probe immersed in plasma is investigated experimentally and theroetically. The depletion of charged particle is characteristic in high pressure plasma in which the mean free path of charged particles is small compared to the probe radius. The mechanism responsible for the depletion is that the density in the vicinity of the probe is decreased by virtue of scattering, according to a simple theory.

However, to obtain a reasonable explanation for the observed depletion, a consideration of another process leading to an additional depletion is needed in addition to the simple theory. The former process is the formation of a disturbed region, which has been discussed extensively in an earlier paper. The existence of a space charge sheath results in a reduction of the depletion.

I. Introduction

Collection of charged particles on a probe immersed into plasma is decreased by a scattering taking place near the probe, even when a space charge sheath is not formed or the probe potential is kept just at the plasma potential. This depletion effect becomes pronounced as the pressure is increased, because of enhancement of the scattering, according to the theories proposed by Kagan[1] and Bohm.[2] Schultz and Brown[3] identified this effect by making comparison between the observed plasma densities by the probe method and the microwave cavity method. They explained the depletion in terms of a decrease of the forward flux due to the scattering in the sheath.

Hereafter, this depletion effect will be investigated experimentally and theoretically, for the purpose of improving reliability of the probe measurement. And the present paper is an extension of the earlier paper which dealt with various sources of error in the probe measurement.[4]

II. Experimental Evidence of the Scattering Effect

In an attempt to verify the depletion, we plot the electron and ion random current densities as a function of the pressure at a constant discharge current. Here, the random electron current density is etimated from the electron current measured at the plasma potential divided by the surface area, while that of ion from the ion current measured at an appropriate negative bias divided by the surface area of the ion sheath, which is computed by use of a corresponding space charge equation.[5]

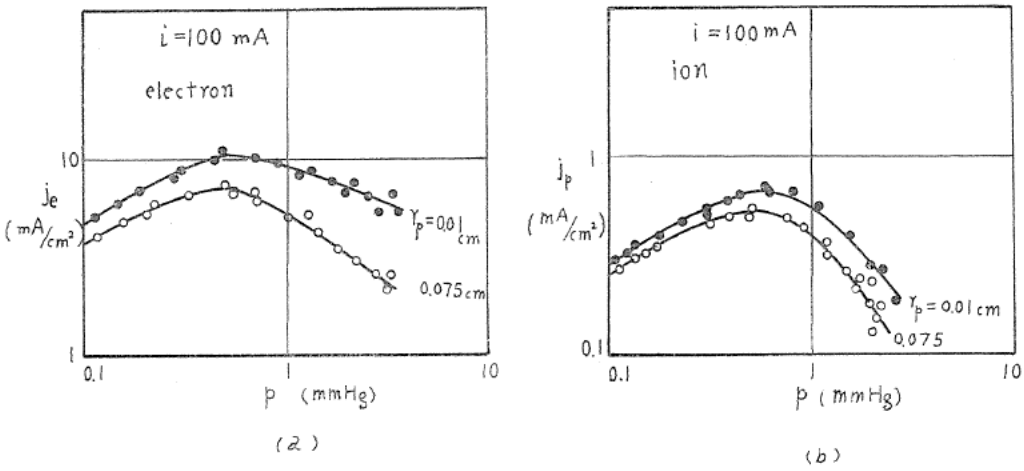

FIG. 1. The random current density v.s. the pressure. (a) electron, (b) ion.

In Fig. 1, a typical example of the plot is shown for Ar. The experiment was carried out using a discharge tube, 3.5 cm in diameter and 35 cm long.

From the figure, it is seen that both the electron and ion random current densities reach at a maximum between 0.1 and 1.0 mmHg. Now, in viewing the figure it should be noted that the plasma density is not kept constant in the measurement, even though the discharge current is kept constant. It is easily understood from a fact that the mobility or the velocity varies with the pressure.

As a rule, the discharge current i is expressed in terms of the density at the tube axis n_0, the mobility at 1 mmHg, the electric E and the pressure p as

$$i \propto n_0 e b_0 (E/p) \quad \text{or} \quad n_0 \propto (E/p)^{-1}.$$

On the other hand, the random current density j_0 is proportional to the plasma density and the mean thermal velocity $\bar{c}$ as

$$j_0 \propto n_0 \bar{c},$$

where $\bar{c}$ is proportional to $(E/p)^{1/2}$. As a consequence, it follows that

$$j_0 \propto (E/p)^{-1/2}.$$

The above relation shows that the random current density which might be evaluated if the depletion is not present can be deduced by extrapolating the plot in lower pressure side to the side of higher pressure, providing that the electric field E is known. In fact, E varies slightly with the pressure as

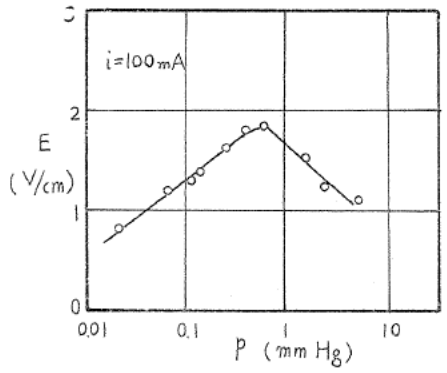

FIG. 2. The electric field v.s. the pressure.

shown in Fig. 2.

Sight of Fig. 1 makes clear that there exists the depletion in the domain of high pressure, and it becomes remarkable as the pressure is increased.

Next, we examine the effect of probe dimension on the depletion. For this purpose, four probes with different diameters are mounted in a plane perpendicular to the tube axis. Figs. 3 (a) and (b) illustrate the dependence of the random current density on the probe diameter for the ion and electron collection, respectively. From the result, we see that the random current density measured by thick probe is less than that by thin probe, and the effect becomes pronounced with increasing pressure.

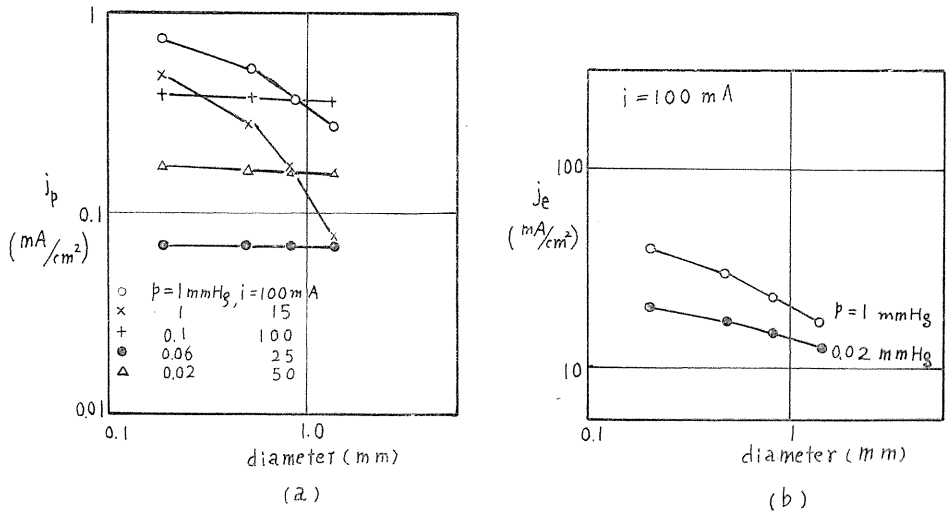

FIG. 3. Dependence of the random current density on the probe diameter.

III. Survey of Theoretical Investigation

Several authors have made a suggestion that the depletion of collection mentioned in the foregoing paragragh is connected with the scattering. The scattering occuring in the proximity of the probe may give rise to a diminishing distribution of density toward the probe. According to a simple theory proposed by Schultz and Brown,[3] the current density reaching the plane probe is

$$J = J_i + J_f - J_b, \tag{1}$$

where J_i is the unscattered particles from the plasma, J_f those particles that have been scattered elastically in the forward direction, and J_b those that have been scattered elastically in the backward direction. Considering that net loss due to the scattering is determined by the collision frequency ν_c, and those current densities are related to each other, they finally obtained the following relation:

$$J = J_d \frac{1}{2} \frac{3 - e^{-\nu_c t}}{1 + \nu_c t}, \tag{2}$$

where J_d is the current density of particles entering the sheath from the plasma and t the time spent in the sheath. Eq. (2) was transformed into the following expression to show the depletion factor:

$$\alpha = J/J_d = \frac{1}{2}\frac{3-e^{-Cp}}{1+Cp}. \tag{3}$$

where C is considered to be constant by them and p donotes the pressure. This expression was employed to discuss the depletion of collection when a positive ion sheath was present. However, from the point of view that the time spent in the ion sheath is not considered to be constant when the pressure is changed as in their experiment, and that the scattering may take place even in plasma, their treatment seems to be not rigorous. However, it is noted that the first persons who identified the depletion were Schultz and Brown.

Kagan treated theoretically the same problem for spherical probe kept at the plasma potential, considering the screening effect, which is not encountered in the plane probe case.[1] He made the assumptions that the elastic scattering was isotropic, the velocity distribution was not changed after scattering and there was no recombination in the space considered.

The current density reaching the probe may be diminished by both the scattering and the screening effect, which is caused by a fact that the particle scattered from the opposite side of the probe has no contribution to the particle density on the side considered.

He started with the following equation determining the particle flux:

$$v\nabla\rho = \frac{1}{\tau}\left\{\int\rho\frac{d\theta}{4\pi} - \rho\right\}, \tag{4}$$

where v is the particle velocity, τ the life time or the reciprocal of the collision frequency, θ the angle between the radial vector and the direction of the velocity and ρ the particle flux per unit angle.

The resultant expression for the particle density at a radius r was given by

$$n(r) = \left[\frac{\cos\theta_r}{2} + \left(1-\frac{r_p}{r}\right)\right]\frac{n_\infty}{1+\frac{3}{4}\frac{r_p}{\lambda}}, \tag{5}$$

where r_p is the probe radius, $\theta_r = \sin^{-1}(r_p/r)$, λ the mean free path of the particle and n_∞ the particle density at infinite radial distance. Also, the depletion factor was thus obtained as

$$\alpha = \frac{1}{1+\frac{3}{4}\frac{r_p}{\lambda}}. \tag{6}$$

Bohm analysed the same problem for spherical probe held at the plasma potential,[2] using an approach that the current entering the probe was determined by the diffusive current just at the surface one mean free path apart from the probe surface. With this approach, the current density j is

$$j = \frac{\lambda \bar{c}}{3} \operatorname{grad} n, \tag{7}$$

where $\bar{c}$ is the root mean square velocity of the particle.

Using the treatment analogous to electrostatics he found the following expression for the depletion factor:

$$\alpha = \frac{\lambda}{r_p}\left(1+\frac{\lambda}{r_p}\right)\Big/\left(1+\frac{\lambda}{r_p}+\frac{\lambda^2}{r_p^2}\right). \tag{8}$$

When the limiting values of α for infinitesimal λ in both cases, eqs. (6) and (8), are calculated, we find $4/3(\lambda/r_p)$ and λ/r_p, respectively. Fig. 4 shows that both plots are numerically not different from others.

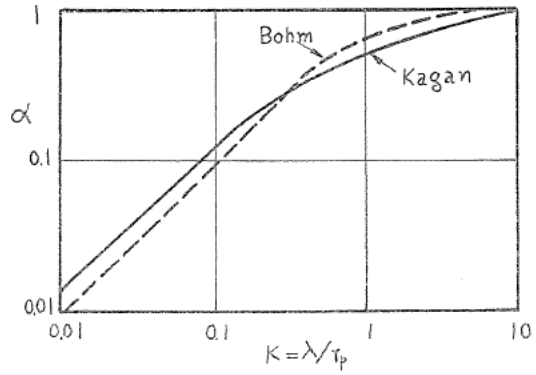

FIG. 4. The depletion factor for spherical probe as a function of $K=\lambda/r_p$. The solid line shows Kagan's and the dotted line Bohm's result.

IV. Depletion Factor for Cylindrical Probe

We shall evaluate the depletion factor for cylindrical probe with Kagan's and Bohm's approaches. The analysis for cylindrical configuration is not simple because of its finite dimension, that is to say, the existence of end effect. For simplicity, we ignore the end effect in the analysis. We also assume a two dimensional model in order to remove mathematical complexity. In this model, contribution of scattering from the axial direction is negleted in computing the particle flux. In this sense, the following formulation of the problem is only an approximation. Further assumtions are made; (1) no electric field exists, (2) distribution of ionization is invariant near the probe, (3) no recombination occurs and (4) elastic scattering is isotropic.

Following Kagan's treatment, the flux density of the particl ρ having velocity v is expressed by the following equation;

$$v\nabla\rho = \frac{1}{\tau}\int\left\{\rho\frac{d\theta}{2\pi} - \rho\right\}, \tag{9}$$

where the scattering occuring within angle $d\theta$ is considered. Also, let us assume

that the velocity v is single-valued in the following analysis. When the relation $\lambda = v\tau$ is used, and the gradient of the particle flux per unit angle along the direction of motion is taken, we find

$$d\rho_v/dl = (1/\lambda)\left\{\rho_v \frac{d\theta}{2\pi} - \rho_v\right\} \tag{10}$$

Expressed in cylindrical coordinate and provided $\partial\rho/\partial z = 0$, we obtain

$$\frac{\partial\rho}{\partial r}\cos\theta - \frac{\partial\rho}{\partial\theta}\frac{\sin\theta}{r} = \frac{1}{\lambda}(B-\rho), \tag{11}$$

where

$$B(r) = \int \rho(r,\ \theta)\, d\theta/2\pi. \tag{12}$$

As a boundary condition, we take

$$\rho(r_p,\ \theta) = 0, \qquad \theta < \pi/2. \tag{13}$$

Now we use three variables as follows;

$$n(r) = \int \rho(r,\ \theta) d\theta, \tag{14}$$

$$H(r) = \int \rho(r,\ \theta) v\cos\theta d\theta, \tag{15}$$

$$K(r) = \int \rho(r,\ \theta)\cos^2\theta d\theta. \tag{16}$$

Multiplying eq. (11) by $d\theta$ and integrating it over all angles, we find

$$\frac{dH}{dr} + \frac{H}{r} = 0. \tag{17}$$

Also, in a similar way we obtain the following equation by multiplying eq. (11) by $\cos\theta d\theta$ and integrating it over all angles;

$$\frac{dK}{dr} + \frac{1}{r}(2K - n) = 0. \tag{18}$$

The solution of eq. (17) is

$$H = -F/2\pi r, \tag{19}$$

where F is the total flow to the probe.

The existence of the screening necessitates to consider ρ inside and outside θ_r individually, where $\theta_r = \sin^{-1}(r_p/r)$. These are

$$\rho(r,\ \theta) = \rho_1(r), \qquad \theta < \theta_r, \tag{20}$$

$$\rho(r,\ \theta) = \rho_2(r), \qquad \theta > \theta_r, \tag{21}$$

For the same reason, the density n is composed of two parts as

$$n(r) = n_1(r) + n_2(r), \tag{22}$$

where

$$n_1 = 2\,\rho_1 \int_0^{\theta_r} d\theta = 2\,\rho_1 \theta_r, \tag{23}$$

$$n_2 = 2\,\rho_2 \int_{\theta_r}^{\pi} d\theta = 2\,\rho_2 (\pi - \theta_r). \tag{24}$$

Also we obtain for H

$$H = \int \rho(r,\ \theta) v \cos\theta d\theta = 2\int_0^{\theta_r} \rho_1 v \cos\theta d\theta + 2\int_{\theta_r}^{\pi} \rho_2 v \cos\theta d\theta$$
$$= 2\,v \sin\theta_r \cdot (\rho_1 - \rho_2). \tag{25}$$

Since

$$\rho_1(r_p) = 0,\ \theta_{r_p} = \pi/2 \text{ and } n(r_p) = n_2(r_p) = 2\,\rho_2(r_p)\,\pi/2 = \rho_2(r_p)\,\pi, \tag{26}$$

H at r_p is given by

$$H(r_p) = -2\,v\rho_2 = -\frac{2\,v}{\pi} n(r_p). \tag{27}$$

Similarly, using eqs. (20) to (25), we find for K

$$K(r) = \pi\rho_2 + 2\{(1/4)\sin 2\,\theta_r + \theta_r/2\}(\rho_1 - \rho_2). \tag{28}$$

Turning back to eqs. (23) and (24), the sum leads to

$$n(r) = 2\,\pi\rho_2 + 2\,\theta_r(\rho_1 - \rho_2). \tag{29}$$

Combination of eqs. (25) and (29) yields

$$2\,\pi\rho_2 = n(r) - \theta_r H(r)/v \sin\theta_r. \tag{30}$$

As a result, K is

$$K(r) = n(r)/2 + \frac{H(r)}{2\,v}\cos\theta_r. \tag{31}$$

Substituting eq. (31) into eq. (19), we get

$$(\lambda v/2)\frac{dn}{dr} + (\lambda/2)\,d/dr(H\cos\theta_r) + (\lambda/r)\cos\theta_r \cdot H = -H. \tag{32}$$

After introducing eq. (19) into eq. (32), we have

$$\frac{dn}{dr} = \frac{F}{v}\left[\frac{(r^2 - r_p^2)^{1/2}}{\pi v r^3} + \frac{1}{\pi r\lambda} + \frac{1}{2\,\pi}\left\{\frac{1}{r(r^2 - r_p^2)^{1/2}} - \frac{(r^2 - r_p^2)^{1/2}}{r^3}\right\}\right] \tag{33}$$

When eq. (33) is integrated with respect to r, the expression for n is finally obtained. Thus, we have

$$n = \frac{F(r^2 - r_p^2)^{1/2}}{2\pi v r^2} + \frac{F}{\pi v}\left[\frac{(r^2 - r_p^2)^{3/2}}{2 r_p^2 r^2} - \frac{(r^2 - r_p^2)^{1/2}}{2 r_p^2} + \frac{1}{2 r_p}\cos^{-1}\frac{r_p}{r}\right] + \frac{F}{\pi\lambda v}\ln r + C. \quad (34)$$

Let us assume that n at a radial distance l which is arbitrary ($l \gg r_p$), as an approximation is n_∞. With such assumption, the integral constant C is found to be

$$C = n_\infty - \frac{F}{2\pi v l} + \frac{F}{\pi v}\left(\frac{1}{2l} - \frac{\pi}{4 r_p}\right) - \frac{F}{\pi\lambda v}\ln l. \quad (35)$$

Consequently, eq. (34) results in

$$n(r) = \frac{F}{2\pi r}\left(\frac{(r^2 - r_p^2)^{1/2}}{r^2} - \frac{1}{l}\right) + \frac{F}{\pi v}\left\{\frac{(r^2 - r_p^2)^{3/2}}{2 r_p^2 r^2} - \frac{(r^2 - r_p^2)^{1/2}}{2 r_p^2} + \frac{1}{2 r_p}\cos^{-1}\frac{r_p}{r} - \frac{\pi}{4 r_p} + \frac{1}{2l}\right\} - \frac{F}{\pi\lambda v}\ln(l/r) + n_\infty. \quad (36)$$

Hence, the density at $r = r_p$ is

$$n(r_p) = -\frac{F}{2\pi v} + \frac{F}{\pi v}\left(\frac{1}{2l} - \frac{\pi}{4 r_p}\right) - \frac{F}{\pi\lambda v}\ln(l/r_p) + n_\infty. \quad (37)$$

On the other hand, eq. (27) leads to

$$H(r_p) = -\frac{2v}{\pi} n(r_p). \quad (38)$$

Combination of eqs. (19) and (38) enables us to find $n(r_p)$ an

$$n(r_p) = \frac{F}{4 r_p v}. \quad (39)$$

Equating eqs. (37) and (39) allows us to obtain the total flow F and the depletion factor α as

$$F = \frac{2\pi r_p v n_\infty}{4}\frac{1}{\frac{\pi}{8} + \frac{r_p}{2\lambda}\ln\frac{l}{r_p}}, \quad (40)$$

and

$$\alpha = \frac{1}{\frac{\pi}{8} + \frac{r_p}{2\lambda}\ln\frac{l}{r_p}}. \quad (41)$$

The above expression are not rigorous, because of the ambiguity in the boundary condition, $n = n_\infty$ at $r = l$. When another boundary condition, $n = n(r_p) = F/4 r_p v$ at $r = r_p$ as eq. (39), is taken instead of the former, the integral constant C is replaced by

$$C = \frac{F}{4\pi r_p} - \frac{F}{\pi\lambda r}\ln r_p. \tag{42}$$

However, in this case, the depletion factor can not be obtained. Instead, the rigorous form of the ratio of $n(r)$ to $n(r)$ is drawn from eqs. (34) and (42) as

$$\frac{n(r)}{n(r_p)} = \frac{2r_p(r^2-r_p^2)^{1/2}}{\pi r^2} + \frac{4r_p}{\pi}\left[\frac{(r^2-r_p^2)^{3/2}}{2r_p^2r^2} - \frac{1}{2r_p^2}\left\{(r^2-r_p^2)^{1/2} - r_p\tan^{-1}\frac{(r^2-r_p^2)^{1/2}}{r_p}\right\}\right]$$
$$+ \frac{4r_p}{\pi\lambda}\ln(r/r_p) + 1. \tag{43}$$

In Fig. 5, the variation of n as a function of $x = r/r_p$ is shown, taking $\lambda = r_p/10$ and $\lambda = r_p$ as examples.

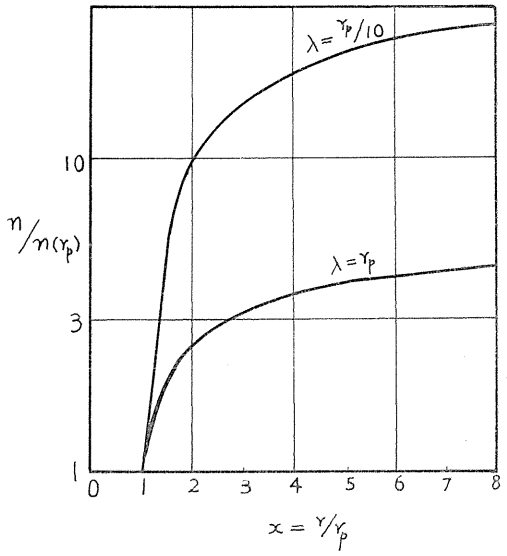

FIG. 5. The density distribution in the vicinity of probe evaluated by eq. (43).

Next, we proceed to find the expression for the depletion factor in accordance with Bohm's analysis. According to his theory, the current density flowing into a probe held at the plasma potential is described by

$$j = \frac{\lambda\bar{c}}{3}\operatorname{grad} n. \tag{44}$$

Since div $j = 0$, eq. (44) turns out to be the Laplace equation $\nabla^2 n = 0$, The current i is

$$i = \int \frac{\lambda\bar{c}}{3}\nabla n dS, \tag{45}$$

where the integral is taken over the surface located one mean free path apart

from the probe surface. As mentioned above, n satisfies the Laplace equation, so that the density n on the probe surface can be found in a way analogous to electrostatics.

Denoting the capacity of electrode as C and the potential as V, we obtain the following equation according to the Gauss theorem;

$$\int \nabla V ds = 4\pi C(V_0 - V_1), \tag{46}$$

where the subscripts 0 and 1 refer to the value at infinite and on the electrode, respectively.

Eq. (45) is written on the analogy of eq. (46) as

$$\int \nabla n dS = 3\, i/\lambda \bar{c} = 4\pi C(n_0 - n_1). \tag{47}$$

Here, C is the capacity of an imaginary electrode with radius of $r_p + \lambda$. Also, $n_0 - n_1$ denotes density difference between the undisturbed plasma and on the probe surface.

On the other hand, the probe current is given by

$$i = \frac{n_1 \bar{c}}{4} A, \tag{48}$$

where A is the surface area of the probe.

Combination of eqs. (47) and (48) yields

$$n = 4\pi\lambda C n_0 / \left(\frac{3}{4} A + 4\pi\lambda C\right). \tag{49}$$

Consequently, the current i is described by

$$i = \frac{n_1 \bar{c}}{4} A = \frac{n_0 \bar{c} A}{4} \cdot \frac{4\pi\lambda C}{(3/4)A + 4\pi\lambda C}. \tag{50}$$

Here, for a cylindrical probe having radius r_p and length L, setting $A = 2\pi r_p L$, $C = 1/2 \ln\{L/(r+\lambda)\}$, we obtain the expression for the probe current as

$$i = (A n_0 \bar{c}/4) \frac{\lambda}{\lambda + \frac{3}{4} r_p \ln\{L/(r_p + \lambda)\}}. \tag{51}$$

Hence, the depletion factor α is

$$\alpha = \frac{1}{1 + \frac{3 r_p}{4\lambda} \ln \frac{L}{r_p + \lambda}}. \tag{52}$$

V. Examination of Experimental Results

As mentioned in Sec. II, the measured random current density as a function of the pressure has a maximum at a certain value of pressure between 0.1 and

1 mmHg for Ar. This may be an apparent evidence for the depletion. Rigorous determination of the depletion factor is made in such a way that the nearly straight plot in low pressure region is extrapolated, the variation of the electric field being taken into account. Thus, the deplation factor is estimated taking the ratio of the actually measured value to the expected one from the extrapolation. In Fig. 6, the depletion factor thus obtained is plotted by the dotted line for Ar, while the thoretical curve basing on eq. (52) by the solid line. Two theoretical curves are drawn for two different values of the mean free path at 1 mmHg, to demomstrate that the discrepancy between the measured and theoretical values may not arise from inappropriate adoption of the value of the mean free path but from other sources. Concerning Ramsauer effect which may influence the mean free path, it is rejective for the discrepancy, in the view that the usual decreasing tendency of electron energy with increasing pressure would lead to an increase of the mean free path and then of the depletion factor, which is not the case.

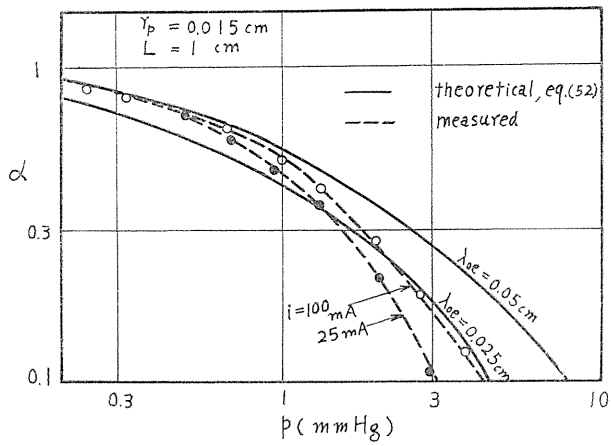

FIG. 6. Comparison between the measured and theoretical values of the depletion factor for electron.

From the point of view that the discrepancy becomes appreciable as the pressure is increased and the discharge current is decreased, it could be interpreted in terms of the formation of a disturbed region extending into the undisturbed plasma, which has been discussed in the earlier paper.

With regard to the effect of probe radius on the depletion factor, an examination of the theory is also made by use of four probes with different radius. The plot shown in fig. 7 is obtained for Ar. In the figure, the experimental results are plotted by the dotted line, whereas the theoretical curves are plotted by the solid line for two different values of the mean free path.

In the case of ion, we obtain a similar plot of the depletion factor, as also shown in Fig. 7. The values of the depletion factor for electron and ion are not apart from each other. However, a striking discrepancy between the experimental and theoretical curves is observed in the case of ion.

A problem arise as to why the depletion for ion is numerically not different

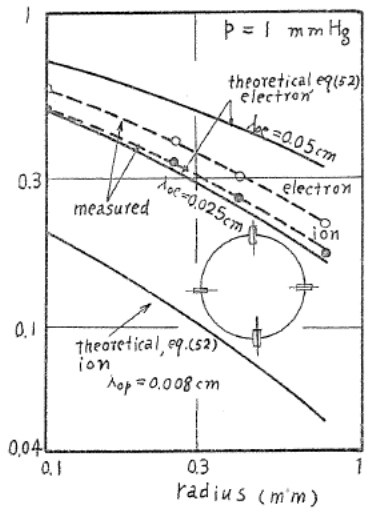

FIG. 7. The depletion factor as a function of the probe radius.

from that for electron in spite of great difference in the mean free path between them. A clue to the understanding of the reason for this fact is to notice that the depletion for electron is measured in the absence of the space charge sheath around the probe, while that for ion in the presence of it. Owing to higher velocity in the space charge sheath, the scattering effect would be less than in plasma. This is equivalent to say that the effective collecting surface moves to a surface far from the probe. Thus, existence of sapce charge sheath results in a reduction of depletion. This is also responsible for the fact that the plot of the depletion factor ceases to decrease at a pressure above several mm Hg, as shown in Fig. 8.

This makes a contrast with the case of the electron. Unfortunately, it is not easy to extend the range of the pressure because of constricting tendency of the discharge column.

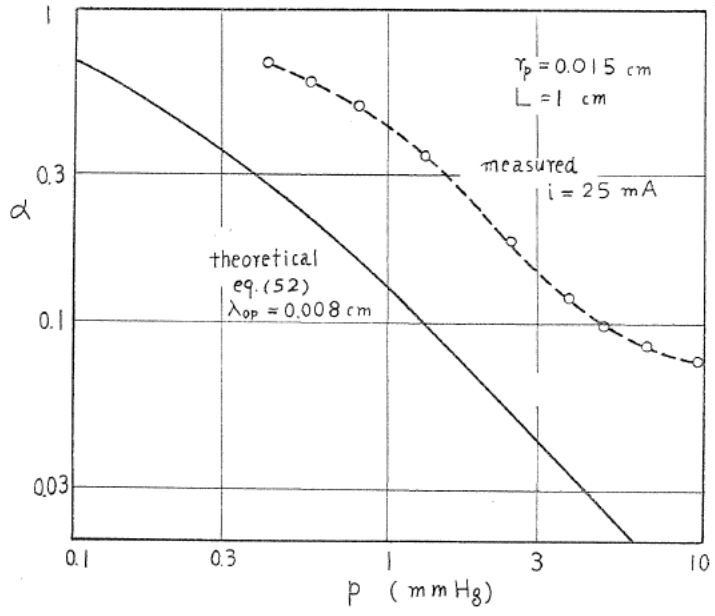

FIG. 8. Comparison between the measured and theoretical values of the depletion factor for ion.

VI. Discussion and Conclusion

The above mentioned scattering effect leading to depletion of the collection on probe is important in estimating plasma density. When this effect is not taken into account, the resulting numerical value of the plasma density would be underestimated by the depletion factor. From the point of view that this effect becomes appreciable as the pressure is raised, the measurement of plasma density by means of the probe method, especially at high pressure, needs for the knowledge of the scattering effect.

The scattering effect in the absence of the space charge sheath was formulated subject to Kagan's and Bohm's treatments and the authors found a similarity between the resultant formulas basing on both the treatments.

However, it was pointed out that there existed an essential distinction between the depletion for ion from that for electron. This is caused by existence of space charge sheath around the probe, which makes the depletion less pronounced by virtue of diminution of scattering in the sheath.

For this reason, the depletion must be computed searately for the regions outside and inside the sheath. As an approximate measure representing the reduction of the depletion due to the existence of space charge, we take

$$\beta = \frac{n(a)}{n(r_p)}, \tag{53}$$

where $n(r_p)$ is given by eq. (37).

Concerning the numerical value of β, it would be greater as the plasma density is lowered or the thickness of sheath is increased. When the scattering effect in sheath must be considered, the situation becomes complicated because the scattering from both outside and inside the sheath may contribute to the density distribution simultaneously. In this case, the knowledge of elastic scattering in higher energy range is needed for the evaluation.

In addition to the scattering, the formation of a disturbed region enhances the depletion, in other words, it gives rise to decrease of density in the vicinity of probe.[4] Such disturbed region develops with decreasing the plasma density and increasing the pressure, so that the discrepancy between the measured value of the depletion factor and that estimated from the theory basing on the scattering becomes large correspondingly.

In our analysis leading to eq. (41), we made the assumption that l is arbitrary. Such penetrating depth can be estimated from the experimental data shown in Fig. 6 and eq. (41). The result shows the value of the penetrating depth is of the order of 10 cm.

Lastly the author is most indebted to Professor K. Yamamoto for many illuminating discussions on the present work.

References

1) Yu. M. Kagan, Zhr. Tekh. Fiz. **24**, 889, 1954.
2) D. Bohm, in "A. Guthrie and R. K. Walkering, The Characteristics of Electrical Discharges in Magnetic Fields", McGraw-Hil, New York, 1949.
3) G. J. Schultz and S. C. Brown, Phys. Rev. **98**, 1642, 1956.
4) T. Okuda and K. Yamamoto, J. Phys. Soc. Japan, **13**, 1212, 1958.
5) T. Okuda and K. Yamamoto, J. Phys. Soc. Japan, **13**, 411, 1958.